Multi-wavelength studies of blazars

Paolo Giommi[*][†]**, Gianluca Polenta, Dario Gasparrini**
ASI Science Data Center c/o ESRIN, via Galileo Galilei, Frascati, Italy

Claudia Monte
Dipartimento di Fisica M. Merlin dell'Università e del Politecnico di Bari, 70126 Bari, Italy
Istituto Nazionale di Fisica Nucleare, Sezione di Bari, 70126 Bari, Italy

We outline the main results of recent extensive multi-wavelength studies of radio, x-ray and γ-ray selected blazars carried out through large observational campaigns involving several space and ground-based facilities, including the *Planck*, *Swift*, and *Fermi* satellites. All observed blazars exhibit the well-known double humped Spectral Energy Distribution (SED), albeit with significant differences in the position of the maxima and in their relative strength. The multi-band selection approach clearly demonstrated that selection effects play a major role in determining the observed properties of blazars. These biases cannot be ignored when drawing conclusions on the physical properties of blazars as a class. The average position of the synchrotron peak of FSRQs is located at approximately 10^{13} Hz in *all* samples, while that of BL Lacs is systematically shifted to higher frequencies, with a distribution that is strongly influenced by the selection method. The observed Compton dominance (CD) also largely depends on the way blazars are discovered, with γ-ray selected FSRQs showing the largest CD values and radio selected objects exhibiting similar power in the synchrotron and inverse Compton components as the most frequent behavior. The multi-frequency emission of most FSRQs is not consistent with simple homogeneous Synchrotron Self Compton (SSC) emission with an observed γ-ray flux often in excess of that predicted by this simple model. However, a surprisingly large fraction ($\approx$ 30-40%) of radio and X-ray selected blazars have not been detected as γ-ray sources even integrating more than two years of *Fermi*-LAT data; the SED of these blazars is consistent with simple SSC models.

---

[*]Speaker.

[†]Report presented on behalf of several Planck, Swift, Fermi and other collaborators

1. Introduction

It is well known that blazars (see e.g. [15] for a review) emit non-thermal radiation across the entire electromagnetic spectrum; however, they do that in a wide variety of ways. The recent concomitant availability of important space-borne facilities, complemented by several ground-based telescopes, is providing an unprecedented opportunity of probing the blazar parameter space with simultaneous observations ranging from radio frequencies to high-energy γ-rays.

In this review we summarize some of the most important results obtained through extensive multi-frequency observational campaigns of sizable samples of objects that probe with good statistics the broad range of multi-frequency properties of blazars.

Details of the observations, many of which have been carried out simultaneously or quasi-simultaneously as a collaborative effort of the *Planck*, *Swift* and *Fermi* teams, are described in [1], [9], and [14]. The multi-frequency data were combined to build the Spectral Energy Distribution (SED) of a large number of blazars belonging to samples with flux limits in the radio, soft-X-ray, hard X-ray and γ-ray bands. These SEDs were then analyzed in order to estimate a number of physical parameters such as the peak of the synchrotron and of the inverse Compton emission, the Compton dominance etc.

2. Blazar SEDs

All the SEDs are presented in detail in [1], [9], and [14]. As an illustrative example Fig. 1 shows the SED of four well-known representative objects, namely 3C 273, BL Lacertae, Mkn 421, and Mkn 501.

This large collection of multi-frequency data show that the SED of blazars is made up of three basic components, namely:

a) non-thermal radiation spanning the entire electromagnetic spectrum, from radio waves to high-energy γ-rays. This component always shows two broad bumps (in $\log\nu$-$\log\nu F(\nu)$ space), the low energy one peaking at energies between the far infrared and the X-ray band, attributed to synchrotron radiation, and the high energy one peaking between the hard X-ray and the γ-ray band, usually attributed to inverse Compton emission on the same synchrotron photons, or to external photon fields such as blue bump, broad line region, torus etc..

b) thermal radiation produced by the accretion process, usually called the blue bump, which is important or dominant at optical/UV frequencies in about 25% of the cases in the samples discussed in ([9]),

c) radiation from the host galaxy which is consistent to be a giant elliptical of absolute magnitude that is approximately constant in all blazars.

Figure 1 illustrates the three spectral components in the SED of four well known objects.

3. SED key parameters

A detailed analysis of the SEDs discussed above allowed [1], [9] to determine the distribution of several parameters, like the spectral slopes in the radio and γ-ray bands, the location and intensity
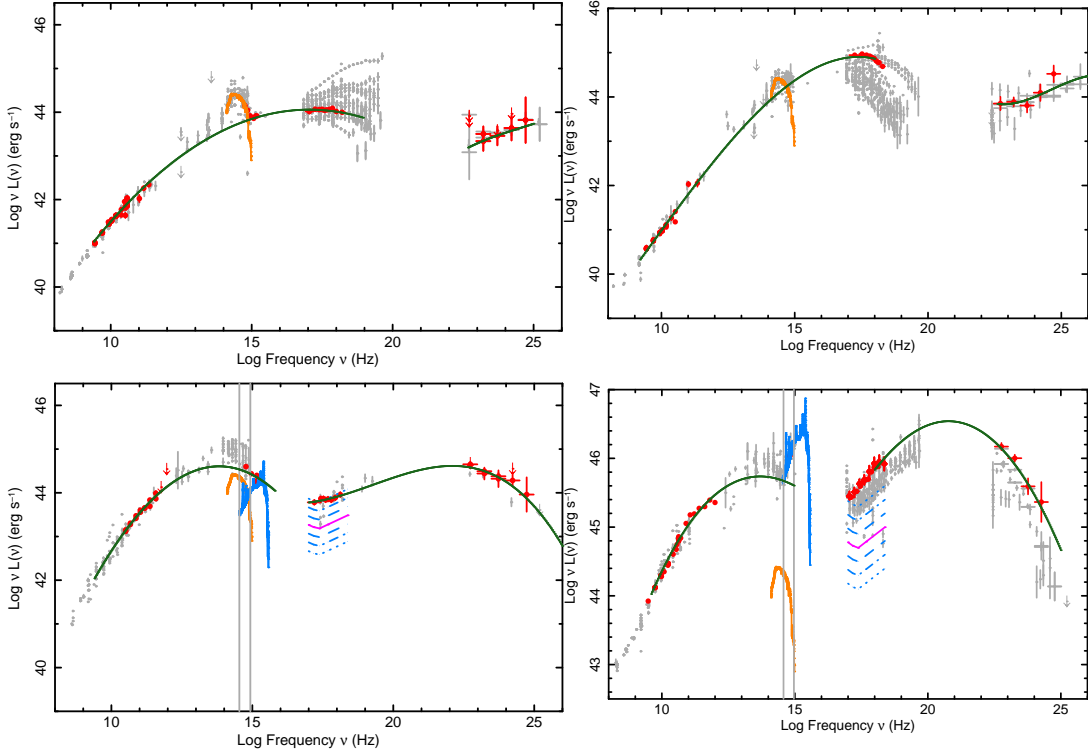
Figure 1: The SEDs of four representative blazars, Mkn 501 (*top left*), Mkn 421 (*top right*), BL Lacertae (*bottom left*), and 3C 273 (*bottom right*), illustrating the three components of Blazar SEDs: i) the emission from the host galaxy (giant elliptical, orange line), ii) the nuclear emission from accretion onto the super-massive black-hole (blue bump/disk emission, blue line); and iii) non-thermal emission from the jet (green lines), which always includes a low energy bump (synchrotron) and a high-energy bump (inverse Compton). Red points represent simultaneous measurements, gray points are archival data. The vertical parallel lines represent the optical window (4 000–10 000 Å).

of the peaks of the synchrotron (ν_{peak}^{S}) and inverse Compton (ν_{peak}^{IC}) components, the Compton Dominance, the relative strength of the thermal (optical radiation from accretion) and the non-thermal components etc.

A number of these parameters, as well as fluxes in different bands, were found to be significantly correlated. As an example Figure 2 shows how the γ-ray spectral index of blazars is correlated with ν_{peak}^{S}. Details of all correlations can be found in [1] and [9].

3.1 SED peak energies

Fig. 3 (top panel) shows the distribution of the rest-frame ν_{peak}^{S} values of FSRQs which is consistent to be the same in all samples considered by [9] and [14] with an average value of $\langle \nu_{peak}^{S} \rangle \approx 10^{13.1 \pm 0.1}$ Hz and a dispersion that is well within one decade. For the case of BL Lacs, instead, (Fig. 3 lower panel) the value of $\langle \nu_{peak}^{S} \rangle$ is at least one order of magnitude larger than that of FSRQs in all samples, and the shape of the distribution strongly depends on the selection method. The distributions of ν_{peak}^{IC} for FSRQs and BL Lacs are also different, but not as much as those of ν_{peak}^{S}. The majority of the sources in all the samples (both FSRQs and BL Lacs) peak between 10^{21}

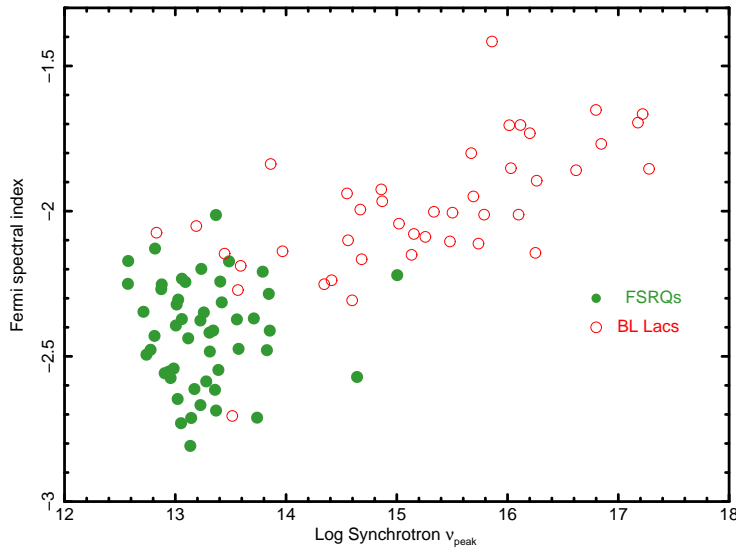**Figure 2:** The γ-ray photon spectral index is plotted against ν^S_{peak} (from [1]). A clear correlation is present, at least for the case of BL Lacs.
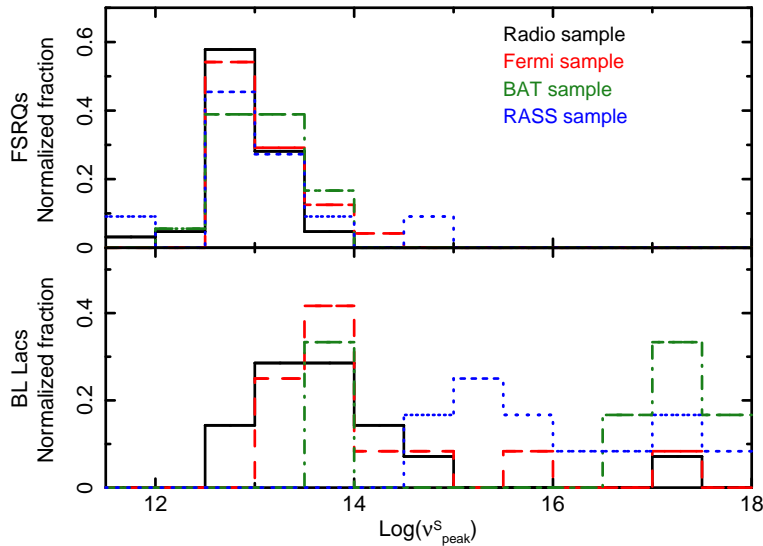

Figure 3: The distribution of rest-frame synchrotron peak energies (ν^S_{peak}) for FSRQs (top panel) and for BL Lacs (lower panel) for all samples considered in [9]

and 10^{23} Hz, with a few extreme HSP BL Lacs reaching $\sim 10^{26}$ Hz (see [9] for details).

3.2 The Compton dominance

One of the most interesting results presented in [9] concerns the distribution of the Compton dominance (CD), that is the ratio between the inverse-Compton and synchrotron peak luminosities. This parameter is of crucial importance for the study of blazar physics, as it is strictly related to the location of the maximum power output in the energy spectrum of a blazar.

The observed CD values range from $\sim$0.3 to $\sim$100. The distributions for different samples are
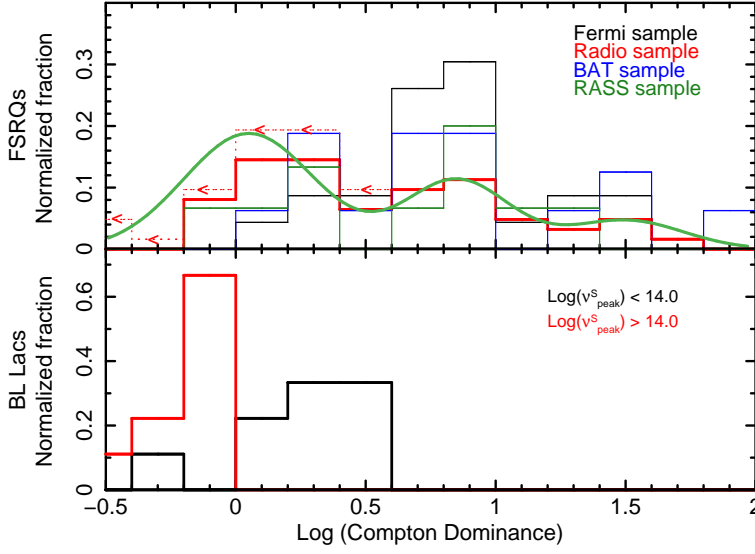
4

Figure 4: The Compton dominance of FSRQs (top panel) and BL Lacs (lower panel) for all blazars samples considered by [9]. Left pointing arrows represent upper limits to the CD of those objects that were not detect by *Fermi*. The green curve is a representation of the possible intrinsic distribution of radio selected (possibly representing the whole population of FSRQs) taking into account of upper limits.

shown in the top panel of Fig. 4 for the case of FSRQs and in the lower panel for the case of BL Lacs.

FSRQs in the *Fermi*-LAT sample, which are γ-ray bright by definition, show a CD distribution peaking at large values, whereas FSRQs selected in the radio and in the X-ray bands, exhibit a distribution that is generally broader and extends to values lower than 1.

In addition, a fraction ranging from $\sim$30% to $\sim$45% of FSRQs in the radio, soft X-ray, and hard X-ray selected samples was not detected by *Fermi*-LAT even in 27 months of exposure. These sources must therefore populate the lower part of the CD distribution. This is shown by the dotted red histogram, which includes the upper limits to the CD, estimated as the ratio of the upper limit to $\nu_{\rm peak}^{\rm IC} F(\nu_{\rm peak}^{\rm IC})$ and the observed value of $\nu_{\rm peak}^{\rm S} F(\nu_{\rm peak}^{\rm S})$ where limits to $\nu_{\rm peak}^{\rm IC}$ and $\nu_{\rm peak}^{\rm IC} F(\nu_{\rm peak}^{\rm IC})$ are obtained by fitting the X-ray data together with the 27-month *Fermi*-LAT upper limits as shown in Fig. 5 for the case of the blazar PKS 0003$-$066.

4. Comparing data with the simplest scenario: homogeneous SSC

In the Synchrotron Self Compton model, when the scattering occurs under the Thomson regime, the peak frequency of the synchrotron ($\nu_{\rm peak}^{\rm S}$) and inverse-Compton ($\nu_{\rm peak}^{\rm IC}$) SED components are related by [1]:

$$\frac{\nu_{\rm peak}^{\rm IC}}{\nu_{\rm peak}^{\rm S}} \simeq \frac{4}{3}\left(\gamma_{\rm peak}^{\rm SSC}\right)^2 \qquad (4.1)$$

where $\gamma_{\rm peak}^{\rm SSC}$ is the Lorentz factor of the electrons radiating at the energy of the peak, and it is related

5

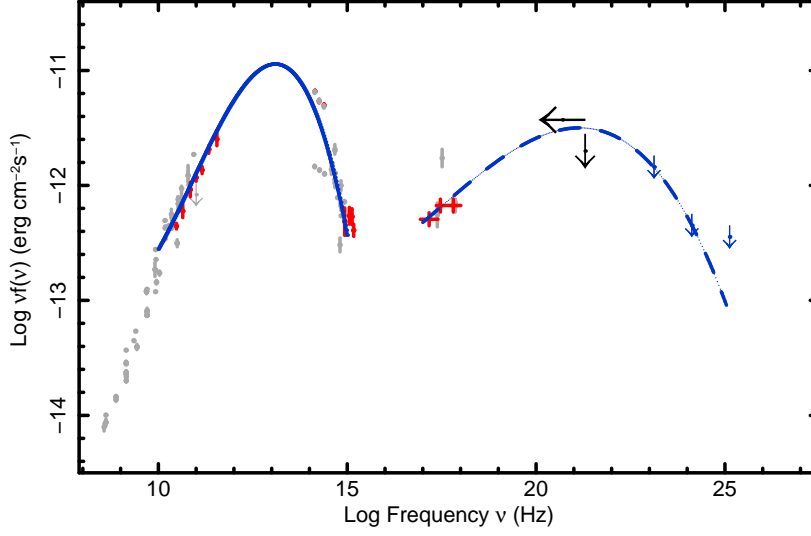**Figure 5:** The SED of the blazar PKS 0003−066, illustrating the estimation of the upper limits on ν_{peak}^{IC} and on $\nu_{peak}^{IC} F(\nu_{peak}^{IC})$ obtained by combining the X-ray data with the 27 month *Fermi*-LAT upper limits (blue arrows).

to the peak frequency of the observed photon spectrum by:

$$\gamma_{peak}^{SSC} \propto \left(\frac{\nu_{peak}^{S}}{B\delta} \right)^{1/2} \tag{4.2}$$

where ν_{peak}^{S} is the rest-frame peak frequency of the synchrotron emission, B is the magnetic field, and δ is the usual Doppler factor (e.g. [15]).

The Thomson approximation is no longer valid when ν_{peak}^{S} is larger than $\approx 10^{15}$ Hz, and the inverse-Compton scattering occurs under the Klein–Nishina (KN) regime.

In Fig. 6 we show the $\log(\gamma_{peak}^{SSC})$, calculated using eq. 4.1, versus the rest-frame $\log(\nu_{peak}^{S})$ for the sources considered in [9]. The solid contour lines define the region of the parameter space for the simple SSC scenario. The transition between Thomson and Klein–Nishina (KN) regimes which happens at $\nu_{peak}^{S} \approx 10^{15}$ Hz has been included in the SSC model using extensive Monte Carlo simulations as explained in [1].

As already found in [1] for the bright γ-ray blazars, only a few of the objects selected in the radio, X, and γ-ray bands considered in [9] are inside or close to the SSC area, implying that simple SSC models cannot explain the SED of most of the blazars observed regardless the different selection criteria. The lack of a strong correlation between radio and γ-ray emission ([9]) is also supporting this conclusion, as it does the fact that the optical/UV spectral slope of the non-thermal emission in some objects is inconsistent with the SSC expectations.

5. γ-ray quiet blazars or simple SSC machines?

As explained above, a significant fraction (30–45%) of FSRQs selected at radio and X-ray frequencies were not seen as γ-ray emitters by *Fermi*-LAT even considering the entire 27 month
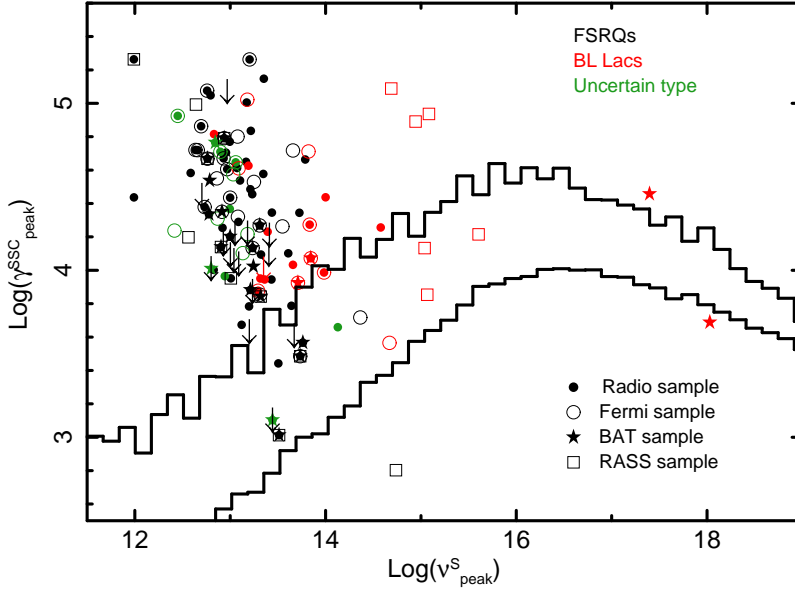
Figure 6: $\log(\gamma_{peak}^{SSC})$ is plotted versus the rest frame $\log(\nu_{peak}^{S})$ for the blazars considered in [9]. The two black solid lines define the area of the parameter space allowed for simple homogeneous SSC models obtained through extensive Monte Carlo simulations.

data set available to [9]. Are these blazars intrinsically γ-ray quiet or their γ-ray emission is just below the *Fermi*-LAT sensitivity limit?

For some of these blazars [9] could obtain limits to ν_{peak}^{IC} (see e.g. Fig. 5) and therefore set upper limits to their γ_{peak}^{SSC}. Many of these values, plotted in Fig. 6 as downward pointing arrows, are close to or inside the region allowed for SSC, hence a simple SSC mechanism is consistent with the observed multi-frequency emission of these objects.

6. The role of selection effects

The choice of considering samples selected in largely different parts of the electromagnetic spectrum (radio, soft X-ray, hard X-ray, and γ-ray) shed light on the strong selection biases that affect physical parameters such as the peak energy of both the synchrotron and inverse-Compton SED components (see Fig. 3) and the Compton dominance (see Fig. 4). Since FSRQs and BL Lacs exhibit different ν_{peak}^{S} distributions, the selection biases must significantly influence the relative abundance of FSRQs, BL Lacs, and of low energy synchrotron peaked (LSP) and high energy synchrotron peaked (HSP) objects.

If there is no correlation between radio flux/luminosity and other parameters such as ν_{peak}^{S}, Compton dominance, etc., selection in the radio band provides unbiased samples that can be used to measure the intrinsic distributions of these important physical parameters.

Selection in the X-ray band strongly favors high-ν_{peak}^{S}/HSP sources as these are much brighter X-ray emitters than LSP sources with the same radio flux. X-ray flux limited samples therefore include a much larger fraction of high-ν_{peak}^{S} BL Lacs than radio-selected ones. This large difference in sample composition is well known ever since the first soft X-ray surveys became available. Recently [10] were able to fully reproduce this difference in samples composition, as well as other
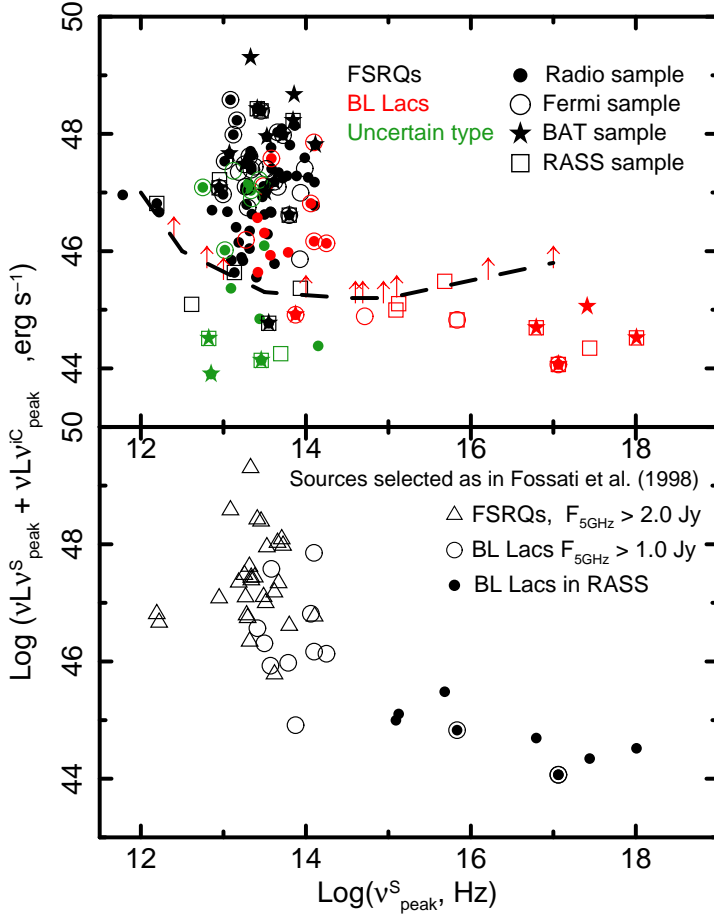
Figure 7: Top panel: The bolometric luminosity of the blazars presented in [9] is plotted against ν^S_{peak}. The bottom panel shows the same plot for the subsample of sources satisfying the selection criteria of [5].

selection effects and diversities in blazar observational properties, through detailed Monte Carlo simulations within a very simple scenario.

Selection in the γ-ray band favors highly Compton-dominated blazars as these are by definition brighter γ-ray sources than those with low Compton dominance for the same synchrotron power. *Fermi*-LAT TS-limited samples favor flat spectrum-high ν^{IC}_{peak} sources (see Fig. 14–17 of [4]), thus explaining the overabundance of both HSP and high CD blazars in *Fermi*-LAT AGN catalogs (e.g., [4]).

7. The blazar sequence

The *Blazar Sequence*, that is a strong anti-correlation between bolometric luminosity and ν^S_{peak} claimed by [5] and [7] has often been the subject of long-standing discussions in the literature (e.g., [8],[12],[2], [11],[13],[6]).

The large set of simultaneous SED data of [9] has been used to test the existence of this relationship. In the top panel of Fig. 7 the logarithm of the bolometric power (that is the sum of the synchrotron and inverse-Compton peak luminosities $L_{Bol} \sim \nu^S_{peak}L(\nu^S_{peak}) + \nu^{IC}_{peak}L(\nu^{IC}_{peak})$) is

plotted versus $\log(\nu_{peak}^S)$. The region of the plot above the dashed line corresponds to luminosities so high that the non-thermal optical light of BL Lacs would completely swamp the emission from the host elliptical galaxy, making the source appear featureless and thus hampering any redshift measurement. The upper limits represent sources with no known redshift and have been estimated assuming that their non-thermal light is larger than ten times that of a giant elliptical host galaxy. No strong correlation is apparent in any of the samples considered. The parameter space seems to be covered with some uniformity with the exception of the area where BL Lacs are expected to have no redshift (top right part of the plot). The bottom panel of Fig. 7 shows the same plot for the subsample of sources that satisfy selection criteria similar to those applied in the paper where the blazar sequence was first reported ([5]), that is FSRQs with $S_{5\,GHz} > 2\,Jy$ and BL Lacs above a very high X-ray flux limit regardless of radio flux, which could be as low as a few mJy. With is particular flux cuts a correlation appears.

Taking into account that

1. different selection criteria introduce significant biases since the distribution of ν_{peak}^S strongly depends on the selection method;

2. the area above the dashed line cannot be populated by blazars with no emission lines, as they would appear completely featureless and therefore without redshift;

3. the particular combination of samples chosen by [5] induces an apparent correlation as in the bottom panel of Fig. 7;

the authors of [9] concluded that the correlation is likely the result of a selection effect. This interpretation is fully supported by the results of the Monte Carlo simulations presented in [10].

8. Conclusions

We have reported some of the results obtained in recent papers presenting multi-frequency studies of large samples of blazars carried out as a collaborative effort of the *Planck*, *Swift* and *Fermi* teams. The main results can be summarized as follows:

- The SED of all blazars observed show the typical double humped shape that is attributed to synchrotron and inverse Compton emission. A large degree of diversity is however observed in samples selected in different parts of the electromagnetic spectrum and between FSRQs and BL Lacs.

- The peak of the synchrotron emission (ν_{peak}^S) in FSRQs is located around 10^{13} Hz and never reaches values larger than $\approx 10^{15.0}$ Hz; its distribution is the same regardless of the way FSRQs are selected. BL Lacs are instead characterized by significantly higher values of ν_{peak}^S in all samples and the shape of the ν_{peak}^S distribution strongly depends on the selection method.

- The observed distribution of the Compton dominance strongly depends on the way blazars are selected. γ-ray selection leads to a distribution that is peaked at high CD values, whereas

radio selection shows a distribution where the maximum frequency is close to equal power in the synchrotron and inverse Compton components.

- Selection effects play a major role in samples composition and induce large biases. Controlling biases is mandatory to understand blazars as a population. In particular the blazar sequence is likely the result of a strong selection effect.

- About 40% of blazars in the radio and X-ray selected samples remain undetected by *Fermi*-LAT after more than 2 years of observing time. This could be a population of γ-ray quiet blazars or simply blazars radiating close to simple SSC.

9. Acknowledgments

References

[1] Abdo A. A., et al., 2010c, ApJ, 716, 30

[2] Caccianiga, A. & Marchã, M. J. M. 2004, MNRAS, 348, 937

[3] Abdo A. A., et al., 2011, submitted to ApJ, (arXiv:1108.1435)

[4] Ackermann M., et al., 2011, submitted to ApJ, (arXiv:1108.1420)

[5] Fossati, G., Maraschi L., Celotti A., Comastri A., Ghisellini G., 1998, MNRAS, 299, 433

[6] Ghisellini, G. & Tavecchio, F. 2008, MNRAS, 387, 1669

[7] Ghisellini, G., Celotti, A., Fossati, G., Maraschi, L., & Comastri, A., 1998, MNRAS, 301, 451

[8] Giommi, P., Menna, M. T., & Padovani, P. 1999, MNRAS, 310, 465

[9] Giommi P., et al., 2011, submitted to A&A, ArXiv:1108.1114

[10] Giommi, P., Padovani, P., Polenta, G., Turriziani, S., DÉlia, V., Piranomonte, S. 2011 A&A, in press ArXiv:1110.4706

[11] Nieppola, E., Tornikoski, M., & Valtaoja, E. 2006, A&A, 445, 441

[12] Padovani, P., Perlman, E. S., Landt, H., Giommi, P., & Perri, M. 2003, ApJ, 588,128

[13] Padovani, P. 2007, Ap&SS, 309, 63

[14] Planck Collaboration 2011, Submitted to A&A ArXiv:1101.2047

[15] Urry C. M., Padovani P., 1995, PASP, 107, 803